Astronomy & Astrophysics

LETTER TO THE EDITOR

The δ Scuti pulsations of β Pictoris as observed by ASTEP from Antarctica

D. Mékarnia[1], E. Chapellier[1], T. Guillot[1], L. Abe[1], A. Agabi[1], Y. De Pra[2], F.-X. Schmider[1], K. Zwintz[3], K. B. Stevenson[4], J. J. Wang[5], A.-M. Lagrange[6], L. Bigot[1], N. Crouzet[7], Y. Fanteï-Caujolle[1], J.-M. Christille[8], and P. Kalas[5, 9]

[1] Université Côte d'Azur, Observatoire de la Côte d'Azur, CNRS, Laboratoire Lagrange, CS 34229, 06304 Nice Cedex 4, France
e-mail: mekarnia@oca.eu
[2] Concordia Station, Dome C, Antarctica
[3] Institut für Astro- und Teilchenphysik, Universität Innsbruck, Technikerstrasse 25/8, 6020 Innsbruck, Austria
[4] Space Telescope Science Institute, Baltimore, MD 21218, USA
[5] Astronomy Department, University of California, Berkeley, Berkeley, CA 94720, USA
[6] Université Grenoble Alpes, CNRS, IPAG, 38 000 Grenoble, France
[7] Instituto de Astrofisica de Canarias, C/via Lactea s/n, 38200 La Laguna, Spain
[8] Fondazione Clément Fillietroz ONLUS, Astron. Observatory of the Autonomous region Aosta Valley, NUS, 11020 (AO), Italy
[9] SETI Institute, Carl Sagan Center, 189 Bernardo Avenue, Mountain View, CA 94043, USA

Received 18 October 2017 / Accepted 11 November 2017

ABSTRACT

Aims. The Antarctica Search for Transiting Extrasolar Planets (ASTEP), an automatized 400 mm telescope located at Concordia station in Antarctica, monitored β Pictoris continuously to detect any variability linked to the transit of the Hill sphere of its planet β Pictoris b. The long observation sequence, from March to September 2017, combined with the quality and high level duty cycle of our data, enables us to detect and analyse the δ Scuti pulsations of the star.
Methods. Time series photometric data were obtained using aperture photometry by telescope defocussing. The 66 418 data points were analysed using the software package Period04. We only selected frequencies with amplitudes that exceed four times the local noise level in the amplitude spectrum.
Results. We detect 31 δ Scuti pulsation frequencies, 28 of which are new detections. All the frequencies detected are in the interval $34.76-75.68\,\mathrm{d^{-1}}$. We also find that β Pictoris exhibits at least one pulsation mode that varies in amplitude over our monitoring duration of seven months.

Key words. stars: individual: β Pictoris – stars: variables: δ Scuti – stars: oscillations – methods: data analysis – techniques: photometric

1. Introduction

With a visual magnitude of 3.8, the A5V star β Pictoris is among the 500 brightest stars in the sky. This star is surrounded by a debris disk composed of dust and gas known to be continuously replenished by evaporating exocomets and colliding planetesimals (Ferlet et al. 1987; Lecavelier Des Etangs et al. 1996; Beust & Morbidelli 2000; Wilson et al. 2017), and hosts at least one planet, β Pictoris b, detected with the Very Large Telescope's (VLT) adaptive optics NaCo system (Lagrange et al. 2009, 2010). The disk, which is seen edge-on, offers a unique opportunity to study the planet-forming environment and planet-disk interactions.

Many studies have been devoted to the physical characterization of the environment of the star. Studies of β Pictoris itself have mainly focussed on the determination of its basic parameters and age (Lanz et al. 1995; Crifo et al. 1997; Di Folco et al. 2004). Crifo et al. 1997 found that the star is very close to the zero age main sequence (ZAMS), which is a finding confirmed by studies of the age of the β Pictoris moving group, 23 ± 3 Myr (Mamajek & Bell 2014).

Very low-amplitude periodic variations in brightness, radial velocity, and line profile have been reported and studied (Koen 2003; Koen et al. 2003; Galland et al. 2006). These observations showed that β Pictoris is one of the brightest known δ Scuti stars. Using photometric time series with a 50 cm telescope, Koen 2003 identified three frequencies with amplitudes below 1.5 mmag, while 18 frequencies were identified from line-profile spectroscopic variations obtained with the SAAO 1.9 m telescope (Koen et al. 2003).

Since its discovery in 2003, the monitoring of the astrometric position of the planet β Pictoris b has provided a good estimation of its orbital parameters. It appears that the orbit of β Pictoris is very close to the transit configuration. As a consequence, it is certain that the Hill sphere of β Pictoris b transits the star with a closest approach either in August 2017 (Wang et al. 2016), October 2017 (Lagrange, in prep.), or January 2018 (Lecavelier des Etangs & Vidal-Madjar 2016). This has motivated a monitoring campaign, started in 2017 and still ongoing, to detect any variability of β Pictoris due to circumplanetary material surrounding its planet (see e.g. Stuik et al. 2017).

In this Letter, we analyse a long-sequence photometric observation, part of the monitoring campaign, of β Pictoris. These observations allow us to better characterize the pulsations of the star. Section 2 of the paper describes the observations and data reduction while Sect. 3 focusses on the frequency analysis. Results are discussed in Sect. 4 and concluding remarks are made in Sect. 5.

2. Observations and data reduction

Photometric observations were made with the Antarctica Search for Transiting Extrasolar Planets (ASTEP) 400 mm telescope, installed at the Concordia station, Dome C, Antarctica (Abe et al. 2013; Guillot et al. 2015; Mékarnia et al. 2016). Briefly, ASTEP 400 is a custom 400 mm Newtonian telescope equipped with a 5-lens Wynne coma corrector and a $4k \times 4k$ front-illuminated FLI Proline KAF 16801E CCD with a 16 bits analogue-to-digital converter. The corresponding field of view is $1° \times 1°$ with an angular resolution of $0.93''$ pixel^{-1} (see Daban et al. 2010, for details).

β Pictoris, which is circumpolar under Dome C latitude, was monitored continuously from the beginning of March through the end of September of the 2017 Antarctic polar campaign; data acquisition started automatically when the Sun was 6 degrees below the horizon. These observations are part of the international campaign dedicated to monitoring the β Pictoris b Hill sphere transit, providing the opportunity to study the circumplanetry material surrounding the planet. β Pictoris is so bright ($M_v = 3.85$ mag) that it saturates our CCD camera even at its minimum exposure time. We therefore used a highly defocussed point spread function (PSF) of approximately 100 pixels in diameter and containing roughly 10^8 counts from β Pictoris. The PSF value was chosen as a compromise between field crowdedness and signal-to-noise ratio compatible with a milli-magnitude precision of each individual calibrated point (considering photon noise only). The β Pictoris stellar field is not very crowded so that the defocussed PSFs of all our reference stars do not overlap with any other nearby stars, which are bright enough to be detected within the exposure time. The Sloan i' filter ($\lambda = 0.695$–0.844μm) was used. We monitored the star continuously when the sky brightness due to the Sun elevation allowed it, at a cadence of ~90 s (exposure time of 60 s, readout, and processing overhead of ~30 s). In parallel, the focussed PSF is tracked by an independent CCD (see Daban et al. 2010) at a cadence of about 1 s. Each acquired science image passes through a custom PSF identification and field recognition algorithm to guarantee the field centring relative to the tracking CCD: the tracking CCD set point is constantly adjusted to compensate small differential drifts between the science and tracking optical paths. Data acquisition was performed automatically. To maximize the recording continuity, we used a reduced exposure time of 30 s when the Sun elevation is between $-6°$ and $-8°$ due to the increased sky brightness.

The ASTEP 400 data reduction pipeline includes bias and dark subtraction, bad pixel masking, and correction of the sky concentration effect, which causes an additive bell-shaped halo component to be present in the centre of each frame (Andersen et al. 1995). We performed aperture photometry of the 18 brightest stars in our images with sufficient counts to be useful. We used the same circular aperture radius for the 18 extracted sources, including β Pictoris and our comparison stars HD 39463 and HD 38891. Figure 1 shows a seven-day subset of the calibrated light curve obtained by ASTEP 400. The rms noise is estimated at 1130 ppm for an integration time of 60 s.
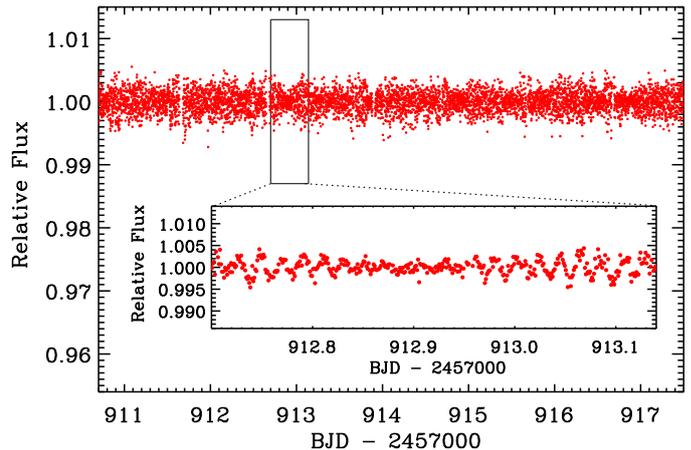

Fig. 1. Seven-day light curve of β Pictoris obtained between 7 and 13 June 2017, showing that data were continuously recorded during that period. The *inset frame* is a zoom-in on an area (~12-h) of the plot, showing the δ Scuti photometric variations of the star.

The comparison data from the *Hubble* Space Telescope (HST) were obtained with WFC3/UVIS in the 953N filter ($\lambda = 0.9532 \mu$m, $FWHM = 0.0064 \mu$m) using spatial scanning mode to avoid saturation (HST programme GO-14621; PI: Wang). Photometry from each spatial scan was extracted using the WFC3 pipeline described in Stevenson et al. 2014, turning each scan into a photometric point with uncertainties dominated by photon noise (57 ppm). The HST data were then corrected for a 0.15% photometric offset between the two scan directions by simultaneously fitting the offset with the δ Scuti pulsations as a quasi-periodic Gaussian process. A detailed analysis of the HST data will be presented in a future publication.

3. Frequency analysis

For our analysis, we kept a data set of 66 418 good measurements (i.e. keeping only data with the Sun below $-8°$ and selecting those obtained under good photometric conditions) collected from March 5, to September 22, 2017, with an average sampling of 90 s. This corresponds to 34.3% of the total time, between the beginning and end of the observing period, and 52.7% of the possible observing time (with the Sun below $-8°$). The frequency analysis was performed with the software Period04 (Lenz & Breger 2005), which is based on classical Fourier analysis and least-square algorithms. We searched for frequencies in the interval 0–200 d^{-1}, but all the δ Scuti frequencies were detected in the spectral region 34.76–75.68 d^{-1}. The relative amplitude of the daily side lobes is kept below 0.4 (Fig. 2) owing to our excellent time coverage, thereby avoiding any ambiguity when extracting each frequency peak.

For each detected frequency the amplitude and phase were calculated by a least-squares sine fit. The data were then pre-whitened and a new analysis was performed. Our analysis was conducted for all frequencies detected with a signal-to-noise amplitude ratio above the widely used value $S/N = 4$ (Breger et al. 1993). We detected 31 δ Scuti frequencies, which are presented in Table 1 and illustrated in Fig. 2. The top panel of the figure shows the amplitude spectrum of our data, including the spectral window based on the times of analysed data, while the bottom panel shows the location of the detected frequencies. We reached a residual noise level of 9.45 ppm in the 35–65 d^{-1} region.
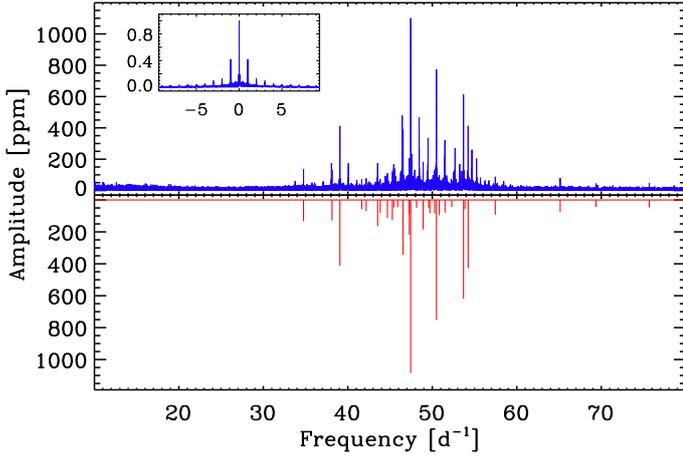
Fig. 2. *Top panel*: amplitude spectrum of the cleaned photometric data of β Pictoris. *The spectral window* is shown in the left corner of the *top panel*. *Bottom panel*: amplitude spectrum with only the detected 31 frequencies resulting from the analysis process.

The uncertainties in the frequencies and their corresponding amplitudes and phases were computed with the relations proposed by Montgomery & O'Donoghue (1999). However, as mentioned in their paper, these uncertainties are underestimates of the true size of the errors. Therefore, the uncertainties given in Table 1 are 3σ errors. We note that the relations proposed by Montgomery & O'Donoghue (1999) give the same error for all amplitudes. We also performed another independent check to investigate the reality of the detected frequencies. We created two equal subsets of the ASTEP time series and analysed these separately. We found a strong match between the frequencies obtained from the two subsets. The fit of the 31-frequency solution is plotted, as an example, over a small set of our measurements and better accuracy HST/WFC3 data points (Fig. 3). The fit is given by the relation $F(t) = 1 + \sum_{j=1}^{31} a_j \sin[2\pi f_j(t - t_0) + \phi_j]$, where $F(t)$ is the relative flux of the star as a function of the time and f_j, a_j, ϕ_j are the detected frequencies, amplitudes, and phases, respectively. The origin of the time is $t_0(\mathrm{BJD_{TDB}}) = 2\,457\,000$. Figure 3 also highlights the complementarity between high accurate and stable HST and the much longer ASTEP data. The agreement is very good. The amplitude of the variations seems to be slightly lower in the HST data, than ASTEP data, which is expected because HST uses a redder filter ($0.9532\,\mu$m instead of $0.7695\,\mu$m).

4. Discussion

All the detected frequencies are confined in the interval between 34.76 and 75.68 d^{-1}. These frequencies are high for a δ Scuti, but not exceptional among hot pre-main-sequence (PMS) δ Scuti star (Casey 2011; Zwintz et al. 2014). The non-regularity of the frequencies in the spectrum is also common for the PMS and ZAMS.

We did not detect any $2f$ frequency. So, all the pulsation modes are sinusoidal, which is consistent with the small amplitudes we observed. We did not detect either $f_i + f_j$ combinations, regular frequency spacing between consecutive eigenmodes, or regular rotational splitting. The rapid rotation of the star ($v \sin i = 130$ km s^{-1}; Royer et al. 2007) certainly breaks any regular pattern in the spectrum (see e.g. Reese et al. 2017).

We looked for amplitude and phase modulation of the first 10 frequencies. We divided the data set into seven parts, each

Table 1. Thirty-one frequencies identified in the amplitude spectrum.

	Frequency (d^{-1})	Amplitude (ppm)	Phase (rad)
f_1	47.43904 ± 0.00005	1084 ± 19	1.994 ± 0.017
f_2	50.49188 ± 0.00007	752 ± 19	4.777 ± 0.025
f_3	53.69138 ± 0.00008	622 ± 19	1.022 ± 0.030
f_4	54.23727 ± 0.00012	429 ± 19	1.477 ± 0.043
f_5	39.06297 ± 0.00012	412 ± 19	2.767 ± 0.045
f_6	46.54281 ± 0.00015	344 ± 19	3.359 ± 0.054
f_7	47.28350 ± 0.00023	216 ± 19	0.077 ± 0.086
f_8	48.91877 ± 0.00027	186 ± 19	0.620 ± 0.100
f_9	43.52749 ± 0.00031	165 ± 19	3.433 ± 0.113
f_{10}	34.76028 ± 0.00038	133 ± 19	3.558 ± 0.141
f_{11}	38.12913 ± 0.00040	128 ± 19	1.683 ± 0.146
f_{12}	45.26910 ± 0.00041	125 ± 19	4.162 ± 0.149
f_{13}	44.68376 ± 0.00046	111 ± 19	0.424 ± 0.168
f_{14}	50.83133 ± 0.00053	95 ± 19	5.271 ± 0.196
f_{15}	57.45220 ± 0.00055	92 ± 19	4.186 ± 0.203
f_{16}	47.27074 ± 0.00056	91 ± 19	5.205 ± 0.205
f_{17}	50.26818 ± 0.00060	85 ± 19	1.093 ± 0.220
f_{18}	49.71224 ± 0.00063	81 ± 19	6.030 ± 0.231
f_{19}	43.82897 ± 0.00064	80 ± 19	3.344 ± 0.233
f_{20}	51.49786 ± 0.00066	77 ± 19	2.491 ± 0.242
f_{21}	65.13460 ± 0.00068	75 ± 19	0.938 ± 0.248
f_{22}	42.17268 ± 0.00074	69 ± 19	3.588 ± 0.271
f_{23}	53.85402 ± 0.00089	57 ± 19	2.518 ± 0.328
f_{24}	41.65042 ± 0.00093	55 ± 19	1.920 ± 0.340
f_{25}	49.55851 ± 0.00104	49 ± 19	3.919 ± 0.382
f_{26}	48.13791 ± 0.00106	48 ± 19	1.010 ± 0.390
f_{27}	45.43672 ± 0.00109	47 ± 19	2.957 ± 0.398
f_{28}	45.90177 ± 0.00113	45 ± 19	5.438 ± 0.414
f_{29}	75.67860 ± 0.00113	45 ± 19	3.357 ± 0.416
f_{30}	69.37515 ± 0.00116	44 ± 19	0.997 ± 0.426
f_{31}	52.30184 ± 0.00116	44 ± 19	5.801 ± 0.427

**Notes.** Each value is presented with its 3σ estimate.

30 days in length, and tracked the amplitude of our 10 highest amplitude peaks through the data set at fixed frequency using least squares. We found an amplitude change for only one pulsating mode that corresponds to our third pulsation frequency ($f_3 = 53.69138$ d^{-1}) (Fig. 4). This amplitude increased from 403 to 826 ± 66 ppm. No significant amplitude variation was found for the other frequencies. On the other hand, no significant phase variation was detected in our analysis. However, the detection of amplitude variations in our seven-month observations is not surprising since 61.3% of the δ Scuti stars observed by the *Kepler* Space Telescope exhibit at least one pulsation mode that varies significantly in amplitude over four years (Bowman et al. 2016).

Koen (2003) and Koen et al. (2003) detected three frequencies (47.4355, 38.0593 and 47.2823 d^{-1}) in their photometric and radial velocity observations with amplitudes a = 1.52, 1.02, 0.88 mmag, and K = 0.129, 0.119, 0.03 km s^{-1}, respectively. Their first and third frequencies correspond to our $f_1 = 47.43904$ and $f_7 = 47.28350$ d^{-1} frequencies but their 38.0593 d^{-1} frequency is clearly a one-day alias of our $f_5 = 39.06297$ d^{-1} frequency. Galland et al. (2006) also detected two of these frequencies in their HARPS measurements f = 47.44 d^{-1}, K = 0.215 km s^{-1} and f = 39.05 d^{-1}, K = 0.17 km s^{-1}.

Koen et al. (2003) searched for periodicity in the moving bumps seen in the broaden line profile of the star. They detected 18 high-degree frequencies between 24.73 and 68.54 d^{-1}.
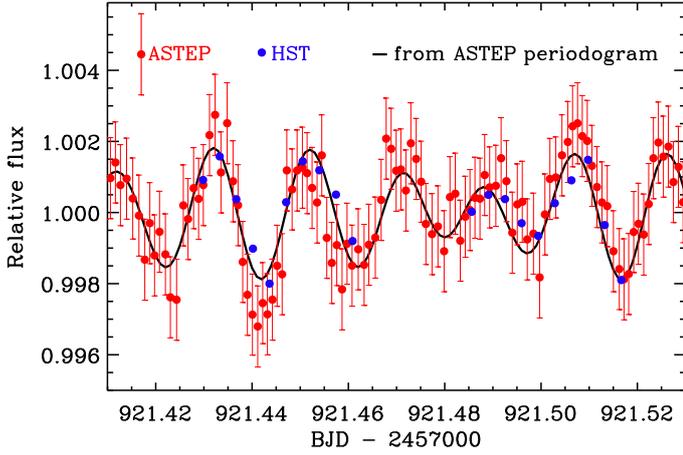
Fig. 3. Comparison between ASTEP 400 (red filled circles) and HST/WFC3 (blue filled circles) photometric measurements of β Pictoris obtained on June 17, 2017. The 1σ values are shown as error bars, which are too small to be seen for HST. The synthetic curve, calculated using our multiple-frequency analysis, is represented as a solid line.
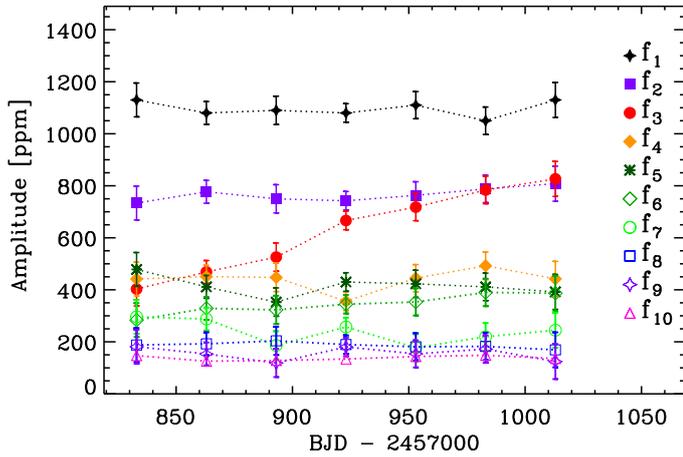
Fig. 4. Amplitude variations of the 10 main frequencies of β Pictoris, showing the amplitude variation of third pulsation mode (f_3 = 53.69138 d^{-1}). The 3σ values are shown as error bars.

Most of these frequencies correspond to high-degree modes ($4 \leq |m| \leq 10$) that cannot be detected in photometry. Only one of their frequencies (45.44 ± 0.02 d^{-1}) was detected in our analysis. It matches our f_{27} = 45.43672 d^{-1} frequency. Koen et al. (2003) provide some mode identifications but, as they discuss, there may be some doubt about the validity of the results. In particular they did not have enough data to avoid the one-day alias in the frequency determination and the fast rotation of the star complicates the problem even further.

5. Conclusions

We have presented and analysed high-precision photometric observations of β Pictoris, covering the period from March to September 2017, using the ASTEP 400 mm telescope installed at Concordia, Dome C in Antarctica. We detected 31 pulsation frequencies among which 28 are new. All of the detected frequencies were in the interval 34.76–75.68 d^{-1}. We found amplitude variation for one pulsation mode, but there was no significant phase change in any detected frequencies.

In this present study, we focussed only on the detection of the pulsation frequencies of the star. A future work will be devoted to the identification of these pulsation modes by combining photometric and radial velocity data. Furthermore, the BRITE-Constellation mission (Weiss et al. 2014) has observed β Pictoris continuously in two colours from November 4, 2016 to June 22, 2017; the corresponding results will be described in Zwintz et al. (in prep.).

The pulsation spectrum, obtained from the ASTEP data, already allows the calculation of a synthetic photometric stellar pulsation curve over a large observation period. This information is crucial to remove the δ Scuti pulsations signal from the β Pictoris light curve to detect signatures of photometric events related either to the Hill sphere transit of β Pictoris b or to any other circumstellar material passing in front of the star.

References

Abe, L., Gonçalves, I., Agabi, A., et al. 2013, A&A, 553, A49
Andersen, M. I., Freyhammer, L., & Storm, J. 1995, in Calibrating and Understanding HST and ESO Instruments, ed. P. Benvenuti, ESO Conf. Workshop Proc., 53, 87
Beust, H., & Morbidelli, A. 2000, Icarus, 143, 170
Bowman, D. M., Kurtz, D. W., Breger, M., Murphy, S. J., & Holdsworth, D. L. 2016, MNRAS, 460, 1970
Breger, M., Stich, J., Garrido, R., et al. 1993, A&A, 271, 482
Casey, M. P. 2011, Ph.D. Thesis, Saint Mary's University, Canada
Crifo, F., Vidal-Madjar, A., Lallement, R., Ferlet, R., & Gerbaldi, M. 1997, A&A, 320, L29
Daban, J.-B., Gouvret, C., Guillot, T., et al. 2010, in Ground-based and Airborne Telescopes III, Proc. SPIE, 7733, 77334T
Di Folco, E., Thévenin, F., Kervella, P., et al. 2004, A&A, 426, 601
Ferlet, R., Vidal-Madjar, A., & Hobbs, L. M. 1987, A&A, 185, 267
Galland, F., Lagrange, A.-M., Udry, S., et al. 2006, A&A, 447, 355
Guillot, T., Abe, L., Agabi, A., et al. 2015, Astron. Nachr., 336, 638
Koen, C. 2003, MNRAS, 341, 1385
Koen, C., Balona, L. A., Khadaroo, K., et al. 2003, MNRAS, 344, 1250
Lagrange, A.-M., Kasper, M., Boccaletti, A., et al. 2009, A&A, 506, 927
Lagrange, A.-M., Bonnefoy, M., Chauvin, G., et al. 2010, Science, 329, 57
Lanz, T., Heap, S. R., & Hubeny, I. 1995, ApJ, 447, L41
Lecavelier des Etangs, A., & Vidal-Madjar, A. 2016, A&A, 588, A60
Lecavelier Des Etangs, A., Vidal-Madjar, A., & Ferlet, R. 1996, A&A, 307, 542
Lenz, P., & Breger, M. 2005, Commun. Asteroseismol., 146, 53
Mamajek, E. E., & Bell, C. P. M. 2014, MNRAS, 445, 2169
Mékarnia, D., Guillot, T., Rivet, J.-P., et al. 2016, MNRAS, 463, 45
Montgomery, M. H., & O'Donoghue, D. 1999, Delta Scuti Star Newsletter, 13, 28
Reese, D. R., Lignières, F., Ballot, J., et al. 2017, A&A, 601, A130
Royer, F., Zorec, J., & Gómez, A. E. 2007, A&A, 463, 671
Stevenson, K. B., Bean, J. L., Madhusudhan, N., & Harrington, J. 2014, ApJ, 791, 36
Stuik, R., Bailey, III, J. I., Dorval, P., et al. 2017, A&A, 607, A45
Wang, J. J., Graham, J. R., Pueyo, L., et al. 2016, AJ, 152, 97
Weiss, W. W., Rucinski, S. M., Moffat, A. F. J., et al. 2014, PASP, 126, 573
Wilson, P. A., Lecavelier des Etangs, A., Vidal-Madjar, A., et al. 2017, A&A, 599, A75
Zwintz, K., Fossati, L., Ryabchikova, T., et al. 2014, Science, 345, 550